SURVIVABILITY • SUSTAINABILITY • MOBILITY
SCIENCE AND TECHNOLOGY
SOLDIER SYSTEM INTEGRATION

TECHNICAL REPORT
NATICK/TR-96/041

AD_____

# DEVELOPMENT OF NEW NONLINEAR OPTICAL MATERIALS FOR APPLICATION TO SENSOR PROTECTION

by

**LARRY R. DALTON**
University of Southern California
Los Angeles California
90089-1661

and

**EDWARD M. HEALY**



September 1996

Final Report

May 1992 - November 1993



Approved for public release, distribution unlimited

**U.S. ARMY SOLDIER SYSTEMS COMMAND**
**NATICK RESEARCH, DEVELOPMENT AND ENGINEERING CENTER**
**NATICK, MA 01760-5000**

**SURVIVABILITY DIRECTORATE**

## DISCLAIMERS

The findings contained in this report are not to be construed as an official Department of the Army position unless so designated by other authorized documents.

Citation of trade names in this report does not constitute an official endorsement or approval of the use of such items.

## DESTRUCTION NOTICE

For Classified Documents:

Follow the procedures in DoD 5200.22-M, Industrial Security Manual, Section II-19 or DoD 5200.1-R, Information Security Program Regulation, Chapter IX.

For Unclassified/Limited Distribution Documents:

Destroy by any method that prevents disclosure of contents or reconstruction of the document.

# REPORT DOCUMENTATION PAGE

*Form Approved*
*OMB No. 0704-0188*



| 1. AGENCY USE ONLY *(Leave blank)* | 2. REPORT DATE | 3. REPORT TYPE AND DATES COVERED |
|---|---|---|
| | Sept 1996 | FINAL - May 1992 to November 1993 |

**4. TITLE AND SUBTITLE**

**Development of New Nonlinear Optical Materials for Application to Sensor Protection**

**5. FUNDING NUMBERS**

DAAK60-92-K-0006

**6. AUTHOR(S)**

**Larry R. Dalton and Edward M. Healy***

**7. PERFORMING ORGANIZATION NAME(S) AND ADDRESS(ES)**

Loker Hydrocarbon Research Institute
Depts. of Chemistry and of Materials Science & Engineering
University of Southern California
Los Angeles, California 90089-1661

**8. PERFORMING ORGANIZATION REPORT NUMBER**

**9. SPONSORING / MONITORING AGENCY NAME(S) AND ADDRESS(ES)**

*U.S. Army Soldier Systems Command
Natick RD&E Center
Kansas St. ATTN: SSCNC-II
Natick, MA 01760-5015

**10. SPONSORING / MONITORING AGENCY REPORT NUMBER**

NATICK/TR-96/041

**11. SUPPLEMENTARY NOTES**

**12a. DISTRIBUTION / AVAILABILITY STATEMENT**

Approved for public release, distribution unlimited

**12b. DISTRIBUTION CODE**

**13. ABSTRACT** *(Maximum 200 words)*

New ladder chromophores were synthesized and characterized for sensor protection applications. A similar effort was carried out for selected metallated pi-electron oligomers. Optical nonlinearity was characterized by both degenerate four-wave mixing (employing both femto- and picosecond pulses) and by pump-probe experiments. Large photo-induced absorption was observed for the new ladder chromophores. In all cases studied, the photo-induced absorption phenomena could be quantitatively described by a three level model. Relaxation to a highly absorbing "gap" state was found to be preferred to direct electron-hole recombination. the relaxation time of the gap state was observed to vary from 40 picoseconds to 10 nanoseconds for various materials studied. The absorption cross section of the gap state was observed to be at least an order of magnitude greater than that of the ground state.

**14. SUBJECT TERMS**

SENSOR PROTECTION PI ELECTRONS
NONLINEAR OPTICAL MATERIALS OPTICAL NONLINEARITY PUMP PROBE
THIRD ORDER NONLINEARITIES DEGENERATE FOUR WAVE MIXING

**15. NUMBER OF PAGES** 47

**16. PRICE CODE**

| 17. SECURITY CLASSIFICATION OF REPORT | 18. SECURITY CLASSIFICATION OF THIS PAGE | 19. SECURITY CLASSIFICATION OF ABSTRACT | 20. LIMITATION OF ABSTRACT |
|---|---|---|---|
| Unclassified | Unclassified | Unclassified | |

CONTENTS

## LIST OF FIGURES

Figure

## LIST OF TABLES

Table

## PREFACE

This report was undertaken by Professor Larry R. Dalton, University of Southern California, Los Angeles, during the period 28 May 1992 to 29 November 1993, under U.S. Army Natick Research, Development and Engineering Center contract DAAK60-92-K-0006. The Natick Project Officer was Dr. Edward M. Healy.

The details of synthesis and characterization of five-ring (PQL) type ladder oligomers have been published in L.R. Dalton, L.S. Sapochak, and L. P. Yu, "Recent Advances in Nonlinear Spectroscopy and Nonlinear Optical Materials," J. Phys. Chem., 97, 2871-83 (1993).

The synthesis and preliminary preparation of metallated materials are described in the publications list that follows. The details of the synthesis are given in the Abstract to Appendix A to this report and the details of degenerate four-wave mixing (DFWM) and pump-probe characterization are given in the thesis of Nansheng Tang, Chapter 5 (University of Southern California, 1994). Femtosecond DFWM and pump-probe measurements have just been completed and support the conclusions of the picosecond work.

The graduate student personnel with partial support associated with this project include Paul Bryson Ph.D., Darin Files, Joyce Laquindanum, Linda Sapochak Ph.D., and Shajing Sun. The postdoctoral fellows were Frederick Strohkendl and Linda Sapochak.

**Publications Derived from Contract Support**

1. L. R. Dalton, "Synthesis of Metallated and Metal-Free π-Electron Polymers for Nonlinear Optical Applications," Polym. Preprints, 33, 371-2 (1992).

2. L. S. Sapochak, F. Strohkendl, L. R. Dalton, N. Tang, J. P. Partanen, R. W. Hellwarth, T. Y. Chang, C. W. Spangler, and Q. Lin, "Excited State Dynamics Studies of Resonance Enhanced Optical Nonlinearity in Ladder Chromophores by Degenerate Four Wave Mixing," in Organic Materials for Nonlinear Optics III (OMNO III), Royal Society of Chemistry, London,1992, pp. 283-8.

3. E.G. Nickel, C.W. Spangler, N. Tang, R.W. Hellwarth, and L.R. Dalton, "Third Order Nonlinearity in Polymer Models and Composites Containing Stabilized Bipolarons." in Organic Materials for Nonlinear Optics III, Royal Society of Chemistry, London, 1992, pp. 237-42.

4. M.L. Sachtleben, C.W. Spangler, N. Tang, R.W. Hellwarth, and L.R. Dalton, "Third Order Nonlinearity in Bis-Ferrocenyl Polyenes." in Organic Materials for Nonlinear Optics III, Royal Society of Chemistry, London, 1992, pp. 231-6.

5. L. R. Dalton, L. S. Sapochak, and L. P. Yu, "Recent Advances in Nonlinear Spectroscopy and Nonlinear Optical Materials," J. Phys. Chem., 97, 2871-83 (1993).

6. L. R. Dalton, L. S. Sapochak, M. Chen, and L. P. Yu "Ultrastructure Concepts of Optical Integrated Microcircuits and Polymeric Materials," in Molecular Electronics and Molecular Electronic Devices. Vol. 2, ed., K. Sienicki (CRC Press, Boca Raton, 1993) pp. 125-208.

7. L. R. Dalton, L. S. Sapochak, and L. P. Yu, "Recent Advances in Nonlinear Spectroscopy," J. Photochem. Photobiol. A, 71, 1-13 (1993).

8. C. W. Spangler, M. Q. He, J. Laquindanum, L. R. Dalton, N. Tang, J. Partanen, and R. W. Hellwarth,"Bipolaron Formation and Nonlinear Optical Properties in Bis-Thienyl Polyenes," Materials Research Society Symposium Proceedings, Vol. 328, Electrical. Optical and Magnetic Properties of Organic Solid State Materials (Materials Research Society, Pittsburgh, 1994) pp. 655-60.

9. C. W. Spangler, P. K. Liu, J. Laquindanum, L. S. Sapochak, L. R. Dalton, and R. S. Kumar, "Incorporation of Ladder Polymer Subunits in Formal Copolymers for Third Order NLO Applications," in Frontiers of Polymer Research, eds. P. N. Prasad and J. Nigam (Plenum, New York, 1993).

10. C. W. Spangler, M. He, E. Nickel, J. Laquindanum, L. R. Dalton, N. Tang, and R. W. Hellwarth, "The Design of New Organic Materials with Enhanced Nonlinear Optical Properties," Mol. Cryst. Liq. Cryst., 240, 17-23 (1994).

11. C. W. Spangler, M. He, P.-K. Liu, E. Nickel, J. Laquindanum, and L. R. Dalton, "The Design of New Organic Materials With Enhanced Nonlinear Optical Properties: Incorporation of Bipolaronic Charge Transfer,"Nonlinear Optics, in press.

12. F. P. Strohkendl, D. J. Files, and L. R. Dalton, "Highly Stable Amplification of Femtosecond Pulses," J. Opt. Soc. Am. B. 11, 742-9 (1994).

# DEVELOPMENT OF NEW NONLINEAR OPTICAL MATERIALS FOR APPLICATION TO SENSOR PROTECTION

## Introduction

In the search for novel organic nonlinear optical materials, mechanisms where new charge states are introduced by either chemical doping or photonic excitation have drawn significant attention.[1-11] In the photonic excitation case, new charge species are created by photo-exciting the originally neutral molecule with a strong laser pulse.[2] In the chemical doping case, the charge species are created by the traditional chemical method: adding another chemical to introduce charge transfer from the original molecule.[2-11] The result of the chemical doping is the generation of either a positive charge or negative charge radical from the original molecule. This chapter concerns two ways of creating a positive radical from an originally neutral molecule: oxidative doping and protonic doping. Even though both methods create positive radicals, there is a basic difference.

The addition of an oxidative agent takes away one or more electrons (we will limit our discussion to the cases when at most two electrons are taken away, namely the polaron and the bipolaron cases). This process is illustrated in Figure 1, where electrons are taken away successively and the molecule goes through a singly charged state (polaron) to eventually the doubly charged state (bipolaron) if excessive dopant is present. Non-resonant polaron and bipolaron state optical properties in some conjugated chain polymers have been studied theoretically by a number of

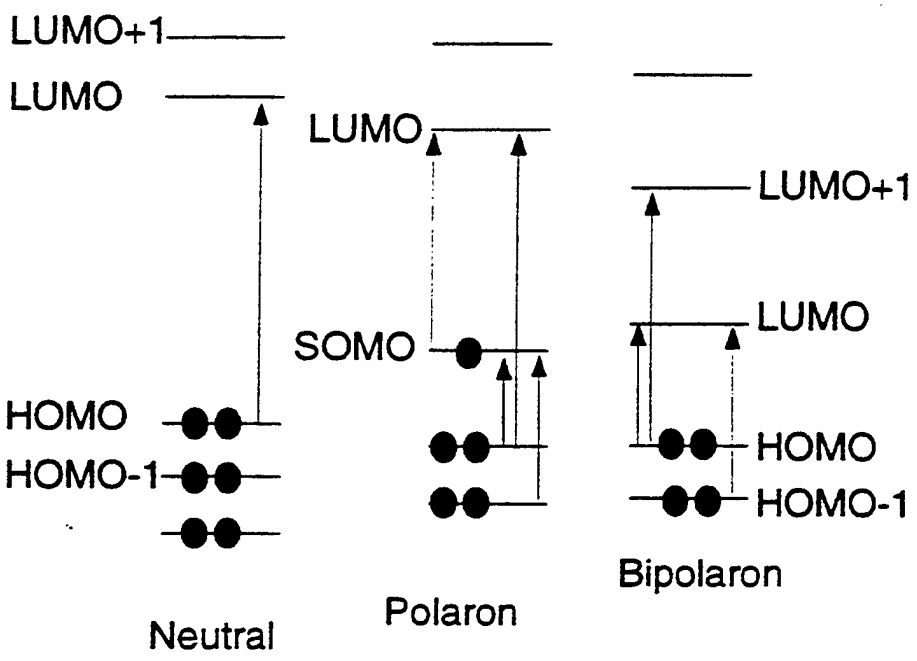


Figure 1. Formation of the polaron and bipolaron state. The abbreviations LUMO, SOMO, and HOMO refer to Lowest-Unoccupied-Molecular-Orbit, Singly-Occupied-Molecular-Orbit, and Highest-Occupied-Molecular-Orbit. As can be seen, the possible transitions move toward lower energies in this sequential doping process.

investigators. Significant enhancement in the third order nonlinearity is predicted.[12-14] However, experimental results are available only in some very limited cases, largely due to the difficulty in synthesizing sequences of long chain polymer with reasonable solubility and stability in common solvents.

Protonic doping is done by adding strong acid to an originally neutral molecule. It normally breaks the pairing of two not bonded electrons in the original molecule and forms some new meta-stable structure. Most of the protonic doping works were done in connection with conducting polymers.[15-19] Optical properties in protonic doped species have been less studied.

In the first half of this report, we study the third order optical nonlinearity of bis-thienyl polyenes (n-BTP) with n=3 to 9 conjugated C=C bonds. The properties of the neutral molecules are studied by the DFWM interferometric method (earlier communication). We determine both the magnitude and the phase of the molecular hyperpolarizability $\gamma_{1111}$ at 532 nm. Our laser frequency of 1.06 μm is well-suited to investigate the doped BTP polyenes. We measure the magnitude of $\gamma_{1111}$ at 1.06 μm and compare it to the calculations from a two-level model in the adiabatic-following regime. Excellent agreement between the calculation and the experiment is obtained. In the second half of this report, we investigate the optical properties of bis-benzothiazole (BBT) by both DFWM and pump-probe techniques. In a sulfuric acid doped bis-benzothiazole sample, we observed a reduction in the transmission of a weak probe beam after a strong pump pulse goes through the sample. This reduction in the transmission has a rise time of ~32 ps and a decay time of ~1 ns. The same characteristic is also observed in DFWM even though across-polarized setting is chosen to eliminate contributions originated from intensity gratings. We interpret this

phenomenon by a three-level model and a selective transition between the two excited-states. We determine some of the parameters involved.

## Optical nonlinearity in bis-thienyl polyenes

We prepare the samples by dissolving powdered bis-thienyl polyenes (BTP hereafter) into methylene chloride (Fisher Scientific, residue after evaporation =0.0004%). The neutral samples in this study have concentrations between $10^{-2}$M to $10^{-4}$M (M=mole/liter). The doping is accomplished by adding 0.1M $SbCl_5$ into the neutral samples. NMR and Electron-Spin-Resonance (ESR or EPR) experiments confirm that the doped samples are in bipolaron state (doubly charged). The neutral samples have colors ranging from light yellow to brown. Upon doping, the samples' colors become darker. The concentrations of the samples are calibrated by comparing the main absorption feature with a predetermined standard.

The structure of the neutral molecules is shown in Figure 2. The thienyl configuration on both ends of the conjugated chain stabilizes the charges and thus the bipolaron state. Samples stable up to several days after doping for longer chains were observed.[9] In our laboratory, we have noticed the decomposition of the bipolaron state in a few minutes after doping for 3-BTP and 4-BTP while the remaining polyenes show increasing stability with longer chains. A possible explanation is the overlapping of the wave function between the two polarons. In shorter chain polyenes, the separation between the two polarons is too short such that significant wave function overlapping occurs. This makes the total energy of the molecule too high to be stable.

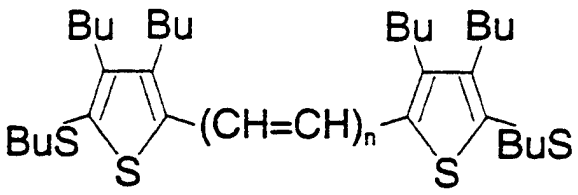


n=3 to 9

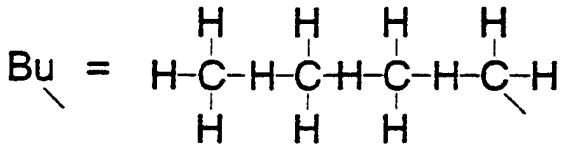


Figure 2. Structure of the neutral bis-thienyl polyenes. The samples in this study contain double bond number from 3 to 9. The five member ring on both ends of the polyenes help stabilizing the polaron pair once they are created.

Some kind of structural relaxation reduces the total energy and at the same time eliminates the bipolaron state.

A typical absorption spectrum is shown in Figure 3 for the case of 8-BTP. The neutral samples all show a triplet absorption maximum varying between 420 nm to 500 nm, while in the doped samples these triplets are bleached out with the simultaneous appearance of a new absorption maximum between 610 nm to 870 nm. The red shift of the absorption maximum is studied in detail by Logdlund *et al.*[6] and by Dannetun *et al.*[7] in a slightly different compound where the end groups are substituted by phenyl. It is understood that this red shift in the absorption maximum is associated with the creation of the bipolaron state.

The DFWM interferometry experiment setup at 532 nm is identical to that described earlier. The doped samples do not show appreciable difference from the solvent in this measurement. The neutral samples all show strong instantaneous signals and small tails except for 3-BTP and 4-BTP, where the DFWM signal decays in about 200 ps. We summarize the magnitude and the phase of the molecular hyperpolarizability $\gamma_{1111}^{exp}$ in Table 1, treating 3-BTP and 4-BTP as if they have instantaneous response. The values are calculated by comparing the DFWM signal at the three-beam-overlap position with that of our $CS_2$ reference. We assume our reference $CS_2$ has a real and positive "chi-three" coefficient $\chi_{1111}^{(3)} = 6.8\times10^{-13} esu$ at 532 nm. Also used in the calculation is the relation $\gamma_{1111}^{exp} = \chi_{1111}^{(3)} / (NL^4)$ where N is the neutral n-BTP molecule number density and L is the local field factor $(n_{re}^2+2)/3$. Due to the small amount of solute in all our solutions, we believe that the refractive index $n_{re}$ is the same as that of the solvent. We use $n_{re} = 1.424$ for the refractive index of the solvent, methylene chloride.

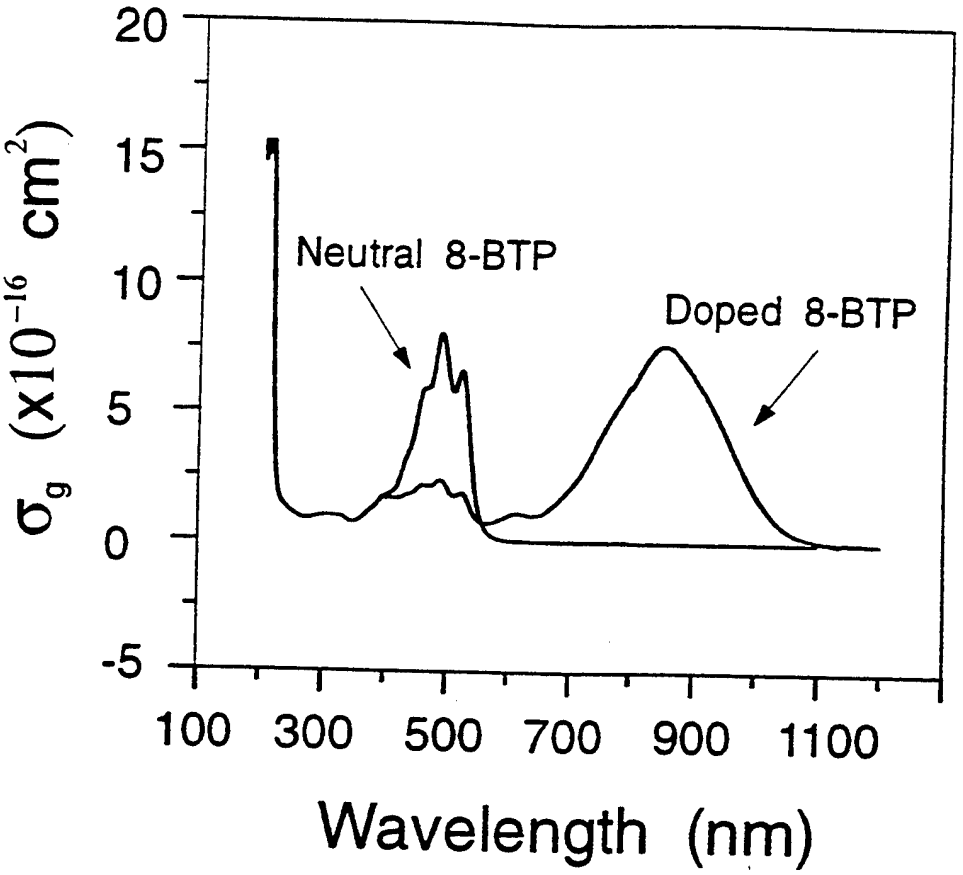


Figure 3. Absorption spectra of 8-BTP. Both the neutral and the doped spectrum is shown. The bleaching of the visible triplet in the neutral sample is accomplished by the appearance of the new peak around 850 nm, a typical feature in doped sample.

The conjugated chain length dependence of the molecular hyperpolarizability $\gamma$ was first studied in an one dimensional system by Hermann *et al.*[20, 21] and Rustagi *et al.*.[22] Their free-electron-in-a-box model shows a power dependence of $\gamma$ on the number of double bonds n,

$$\gamma = an^b \qquad (1)$$

with an exponent close to b=4. Good agreement between theory and experiments were obtained. More recent investigations add electron-electron correlation into the calculation.[23-25] The power law dependence then obtained is in the range b=4.6 to 5.4 for neutral molecules and b=6 for the bipolaron state.[13, 14, 23, 24, 25]

Table 1. $\left|\gamma_{1111}^{exp}\right|$ of neutral bis-thienyl polyenes at 532 nm. Values are obtained by the DFWM interferometric technique. $\varphi^{(3)}$ is the phase of $\chi_{1111}^{(3)}$.

| Sample | 3-BTP | 4-BTP | 5-BTP | 6-BTP | 7-BTP | 8-BTP | 9-BTP |
|---|---|---|---|---|---|---|---|
| $\left\|\gamma_{1111}^{exp}\right\|$ ($\times 10^{-31}$ esu) [a] | 0.66 | 4.9 | 24.5 | 87 | 150 | 510 | 235 |
| $\varphi^{(3)}$ [b] | 151° | 141° | 172° | 164° | 186° | 172° | 158° |

a. Estimated errors are ~±20% relatively and ~±50% absolutely.
b. Estimated errors are ~±10° relatively and ~±20° absolutely.

We show the conjugated double bond number n dependence of the magnitude in the molecular hyperpolarizability $\gamma_{1111}$ in Figure 4. The least square fit to $|\gamma_{1111}|$ at 532 nm in the neutral molecules represented by the center solid line in Figure 4(a) gives

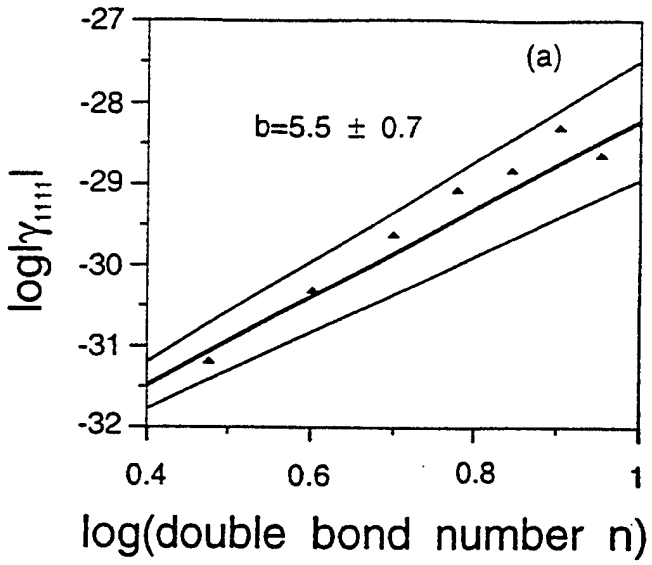


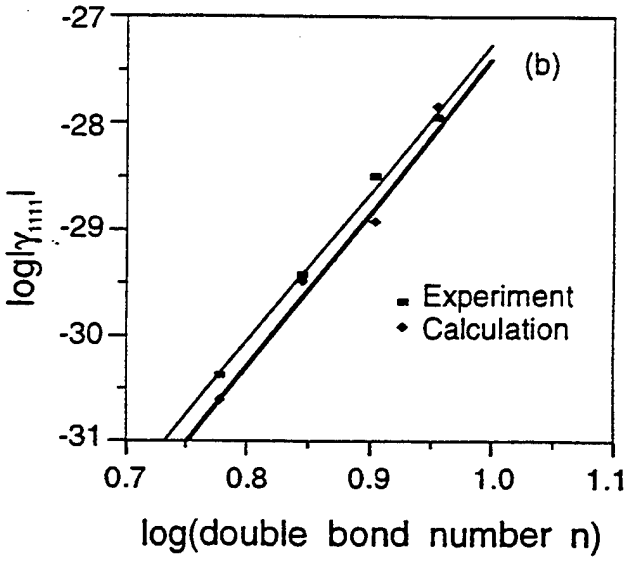


Figure 4. Chain length dependence of the hyperpolarizability. (a) The neutral samples are measured at 532 nm, a wavelength close to the absorption peaks. The solid line represents the best least-square fitting to the data and gives a power law dependence on the number of the double bond with b=5.9. Data uncorrected for resonant enhancement. (b) Both the measurements at 1.06 μm and the two-level model calculation from the absorption data shown. The solid lines are the power law fits. Good agreement between the two-level model calculation and the experiment is apparent.

b=5.5±0.7, a number slightly larger than the previous theoretical calculations. The two thinner lines in Figure 4(a) define the 90% confidence range in b. Our laser wavelength of 532 nm is within the characteristic absorption band of each n-BTP sample. Therefore we believe that the measured $|\gamma_{1111}|$ values contain contributions from resonant enhancement.

At 1.06μm, the DFWM signal of the neutral samples is not distinguishable from that of the solvent.

The doped samples have completely different wavelength dependence in the two laser wavelengths we tried. The filled squares in Figure 4(b) show the DFWM measurements in the doped samples 6-BTP to 9-BTP at 1.06μm. We fit the data to (5-1) as represented by the thinner solid line in Figure 4(b) and find b=14.0±2.6, a number much larger than any theoretical predictions.

We notice that all the aforementioned theoretical calculations were performed in the non-resonant regime while our laser wavelength of 1.06μm sits at the absorption wing of our doped samples. Fortunately the single absorption peak in the doped samples stays far away from any other absorption feature and our laser wavelength at 1.06 μm is far from the maximum. In this case, we believe the bipolaron state can be approximated by a two-level model in the adiabatic-following regime.

Theory predicts for the hyperpolarizability $\gamma_{1111}$ at frequency ω shifted Δ above resonance

$$\gamma_{1111} = \frac{2p_{12}^4}{3(\hbar\Delta)^3}, \qquad (2)$$

if the "adiabatic-following" regime can be assumed,[26] i.e., the frequency spectrum of the laser pulse should not overlap the absorption line much. Here $p_{12}$ is the magnitude of the transition dipole moment between the two levels. We also have the relation between the spontaneous emission decay rate $A_{21}$ from the upper state to the ground state,[27]

$$A_{21} = \frac{4 p_{12}^2 \omega^3}{3\hbar c^3}. \qquad (3)$$

To relate $A_{21}$ to the absorption spectrum, we define a frequency $\nu$ dependent line shape function $g_{21}(\nu)$ that depends on frequency $\nu$ (Hz) and is normalized by

$$\int g_{21}(\nu) d\nu = 1. \qquad (4)$$

Here the integral goes over the range 600 nm to 1200 nm for our doped samples 6-BTP to 9-BTP (We assume the contribution to the integral from the remaining region is insignificant). The absorption cross-section $\sigma$ satisfies the well-known Fuchbauer-Ladenburg formula (assuming equal level degeneracies)

$$\sigma = \frac{\lambda^2 g_{21}(\nu)}{8\pi n_{re}^2} A_{21}, \qquad (5)$$

where $\lambda$ is the wavelength in vacuum.

We start from the absorption spectrum to determine the line shape function $g_{21}(\nu)$ and the absorption cross-section $\sigma$. We then calculate $A_{21}$ from (5-5). Putting

$A_{21}$ into (5-3), we find the dipole moment $p_{12}$. With the help of (5-2), we can derive $\gamma_{1111}$. Table 2 summarizes our calculation using the two-level model in the adiabatic-following regime. We plot these calculated $\gamma_{1111}$ values for 6-BTP to 9-BTP as filled squares in Fig. 5-4(b). The thicker solid line fits these calculated values to (5-1) and gives a value b=14.5±3.1. We believe that the calculated values agree with the experiment values to within experimental error, considering the uncertainty in the absorption data.

Table 2. Nonlinearity of bipolaronic n-BTP polyenes. a) Experimental data obtained with parallel polarizations in DFWM at 1.06 μm. b) Two-level calculation based on the absorption spectra and Eqns. (2) to (5). We estimate the uncertainty in $\left|\gamma_{1111}^{exp}\right|$ and $\gamma_{1111}$ to be 50%.

| | Sample | 6-BTP | 7-BTP | 8-BTP | 9-BTP |
|---|---|---|---|---|---|
| a | $\left\|\gamma_{1111}^{exp}\right\|$(x10$^{-30}$ esu) | 0.42 | 3.8 | 31.9 | 114 |
| b | $\gamma_{1111}$(x10$^{-30}$ esu) | 0.25 | 3.27 | 11.9 | 143 |
| | $\sigma_{1.06\mu}$(x10$^{-17}$ cm$^2$) | 1.13 | 0.237 | 4.48 | 28.3 |
| | $g_{21}(\nu)\|_{1.06\mu}$(x10$^{-16}$ s) | 4.92 | 0.399 | 5.78 | 12.1 |
| | $A_{21}$(x10$^8$ s$^{-1}$) | 1.03 | 2.67 | 3.49 | 10.6 |
| | $p_{12}$(x10$^{-17}$ esu) | 1.99 | 3.20 | 3.66 | 6.37 |
| | $\hbar\Delta$ (x10$^{-13}$erg) | 7.54 | 5.98 | 4.65 | 4.25 |

We now try to justify the "adiabatic following" assumption in the above derivation. In our experiment, our laser pulse has diameter of ~1.6 mm and the total power is roughly 1.2 mJ per pulse with $\delta t$ ~30 ps duration. This gives us a peak power of ~1.76 GW/cm$^2$ or a peak electric field of 1.15x10$^8$ V/cm (38.4 St.V/cm). The Rabi

frequency is $\omega_R = \frac{\mu|E|}{\hbar}$=1.03x$10^{12}$/S. This gives $\omega_R \delta t$=30.8>1. Our laser has a pulse duration of – 30 ps and a bandwidth of – 0.1 THz. The absorption band around 850 nm of the doped n-BTP is about 200 nm wide, or a bandwidth of – 84 THz. We see that the standard adiabatic following condition is satisfied.

**Properties of protonic doped bis-benzothiazole(DBBT)**

The structure of the neutral bis-benzothiazole (BBT) is shown in Figure 5. The BBT/$H_2SO_4$ sample used in this experiment is prepared by dissolving dried BBT powder into 98% pure $H_2SO_4$. We determine the concentration of BBT in the solution to be 2.9x$10^{-3}$M. The sample is contained in a 1 mm spectral photometer cell during our experiments.

UV-visible absorption spectra show the typical red shift of the maximum absorption from 376 nm in the neutral samples to 454 nm in the protonic doped sample. In our experiments, the laser wavelength of 532 nm is at the absorption band edge where the sample has a low intensity transmission of ~0.18. BBT exhibits luminance under illumination of either a UV source or our laser pulse at 532 nm.

NMR experiments indicate that the end group R is substituted by hydrogen atom on both sides upon doping by the sulfuric acid. Combining the result in NMR and EPR, we believe that the ground state protonic doped BBT is a mixture of polaron and bipolaron species with polaron dominance.

Our experimental setup for the DFWM experiment is identical to the ones described above. The temporal response in the DFWM signal is shown in Figure 6 where the data are obtained by delaying either the forward or the backward beam. In

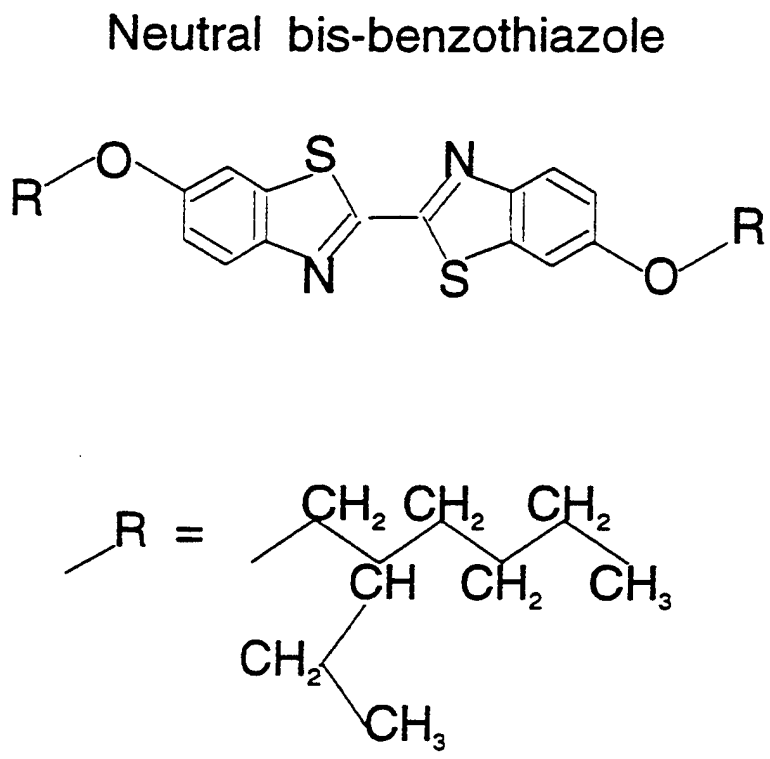


Figure 5. Structure of the neutral bis-benzothiazole (BBT) molecule. Upon doping, the end group R is replaced by hydrogen atom.

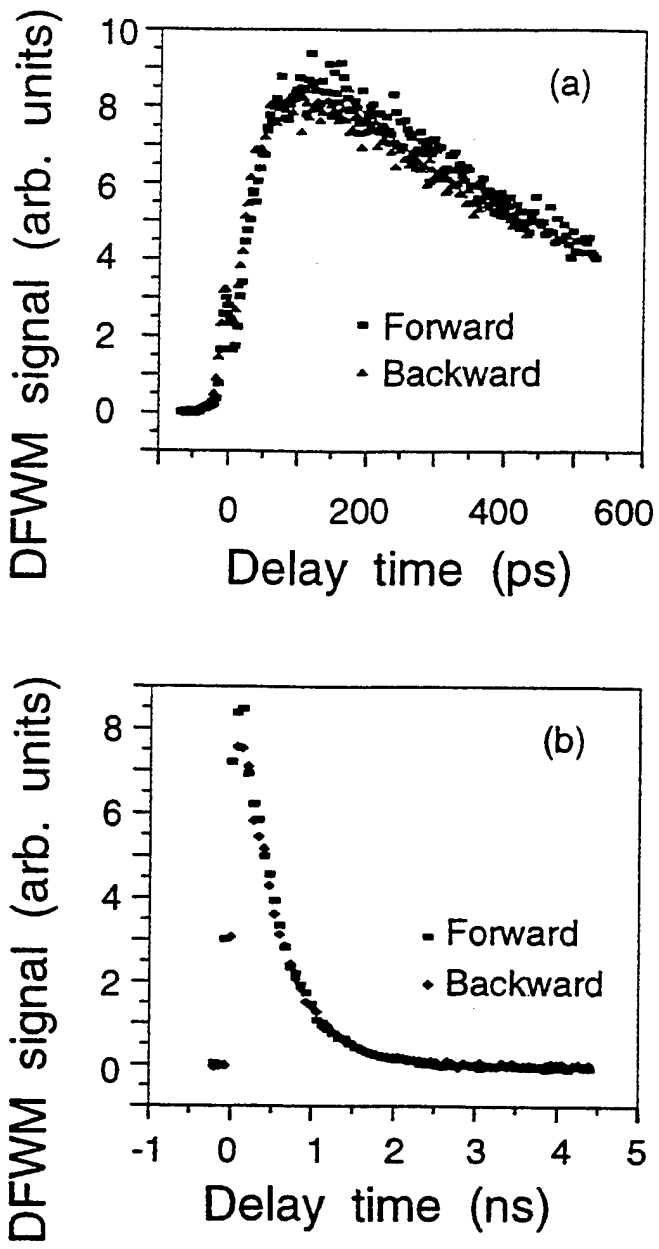


Figure 6. Temporal response of the DFWM signal of the doped BBT. Both forward and backward delay data overlap well in all time. (a) Details around time zero. (b) The longer time response. The data shown are obtained by using cross polarization among the three input beams such that no intensity grating is created inside the sample.

the case when all three input beams have the same polarization, the typical thermal and acoustic features are seen. The data shown in Figure 6 are those with cross polarizations among the beams such that no intensity grating is written by them. The excellent overlapping between the forward and backward data suggests that the data shown do not contain any thermal or acoustic contribution. Otherwise the large difference in the grating spacing between the forward and the backward case would give a very different temporal dependence (we observe this difference when we rotate the polarizers to allow an intensity grating written in the sample). All data show an instantaneous response about three times smaller than the maximum at a delayed time. The DFWM signal builds up and maximizes at about 100 ps after the three-beam overlap position. After that the signal decays back to zero in about 1 ns.

The pump-probe experimental layout is depicted in Figure 7, where a strong pump pulse at 532 nm with pulse duration ~30 ps and fluence up to ~220 mJ/cm$^2$ enters the sample from one side. A weak probe beam P, which we estimate to be hundreds of times weaker than the pump, goes in from the other side and forms a small angle of ~1.5° with the pump beam F. Three polarizers P1 to P3 control the polarization in the pump, the probe, and the transmitted probe. Part of the probe beam P is directed onto a photodiode PD2 by a microslide BS. The transmitted probe beam is reflected by a mirror M into another photodiode PD1 after going through a polarizer P2 and an aperture AP. A set of neutral density filters ND is used to control the pump fluence. The data collected with the pump beam F cross-polarized to the probe beam P are shown in Figure 8, where the pump fluences are written next to the temporal dependence of the transmission. We compare two cases: when the aperture AP is about the size of the probe beam, and when the aperture is fully opened. We find no distinguishable difference in the transmissions. This suggests that the reduction in the

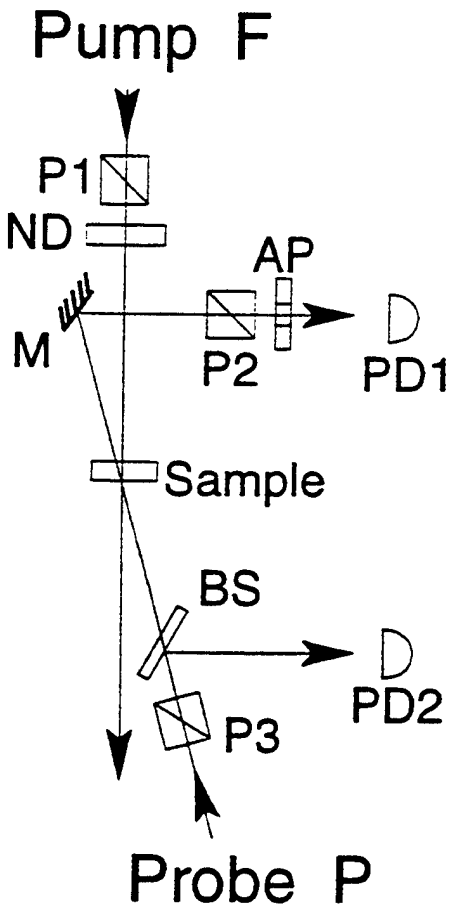


Figure 7. Experimental setup for the transmission measurement. The angle formed by F and P is ~1.5°. Three polarizers P1, P2, and P3 can be independently adjusted. Neutral density filter ND is used to vary the pump fluence. BS is a microslide used to direct part of the probe pulse to photodiode PD2. Another photodiode PD1 is used to measure the transmitted probe beam energy. In front of PD1 we use an adjustable aperture to help distinguish the nature of the reduction in the transmission.

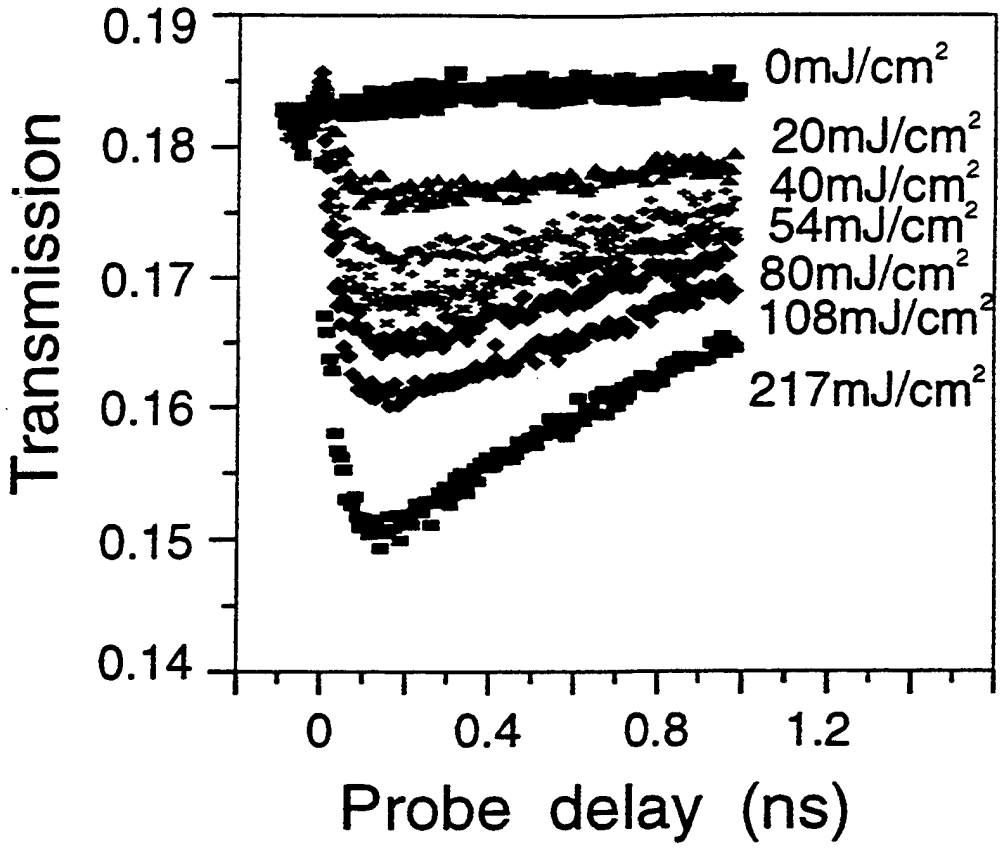


Figure 8. Transmission of the doped BBT at different pump fluence. The temporal dependencies are shown up to −1 ns.

transmission is of absorptive nature. A temporal behavior similar to those of DFWM data is observed.

To interpret the observation in both the DFWM and the pump-probe experiments, we propose a three-level model as illustrated in Figure 9. The pump pulse promotes the doped BBT (DBBT hereafter) molecules from the ground state 0 into the excited state 1 with a number density $n_1$. The DBBT then relaxes back to the ground state with time constant $\tau_0$ or goes into a metastable state 2 with time constant $\tau_1$. Once in state 2, DBBT molecules return to the ground state with a much longer time $\tau_2$. We explain our data in the following ways. The reduction in the transmission of the pump-probe experiment can be attributed to the larger absorption cross-sections $\sigma_1$ and $\sigma_2$ in excited-states 1 and 2 as compared to that of the ground state $\sigma_0$. To understand the DFWM data, we introduce the concept of selective relaxation: the polarization grating written in the sample causes different amount of DBBT participating in the state 1 to state 2 transition and thus creates an absorption grating in the sample. The DFWM signal evolves as the amount of state 2 DBBT changes. We derive the following rate equations among the three states:

$$\frac{dn_1}{dt} = -\frac{n_1}{\tau_1} - \frac{n_1}{\tau_0}, \tag{6}$$

$$\frac{dn_2}{dt} = \frac{n_1}{\tau_1} - \frac{n_2}{\tau_2}, \tag{7}$$

$$N = n_0 + n_1 + n_2. \tag{8}$$

Here N is the total number density of DBBT. With the initial conditions $n_1(t=0) = n_{10}$ and $n_2(t=0) = 0$, we arrive at

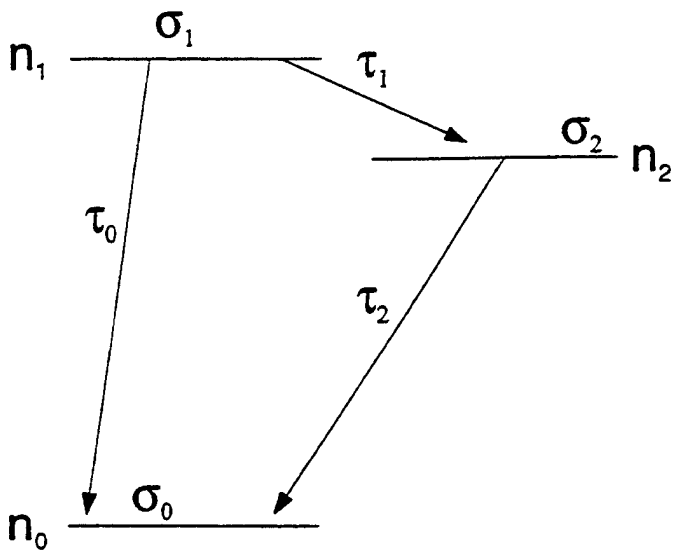


Figure 9. The three-level model for the doped BBT. The pump pulse puts doped BBT into state 1. These excited doped BBT can then decay back to the ground state 0 directly or through a third level state 2.

$$n_1 = n_{10} e^{-t/\tau_{10}}, \qquad (9)$$

and

$$n_2 = n_{20}(e^{-t/\tau_{10}} - e^{-t/\tau_2}), \qquad (10)$$

with the two new constants being $\tau_{10} = (1/\tau_1 + 1/\tau_0)^{-1}$ and $n_{20} = \dfrac{n_{10}}{\tau_1(1/\tau_2 - 1/\tau_{10})}$.

To formulate the pump-probe data, we write the low intensity transmission $T_0$ and the intensity after the pump pulse $T_1$ in the following,

$$T_0 = e^{-N\sigma_0 l}, \qquad (11)$$

$$T_1 = e^{-N\sigma_0 l - n_1(\sigma_1 - \sigma_0) l - n_2(\sigma_2 - \sigma_0) l}. \qquad (12)$$

Here $l$ is the sample thickness. Substituting (9) and (10) into (11) and (12) and redefining time zero to be $t_0$ in our lab clock, we can write

$$\ln(T_1 / T_0) = -a[e^{-(t-t_0)/\tau_2} - (1-b)e^{-(t-t_0)/\tau_{10}}]. \qquad (13)$$

The two new dimensionless constants are defined as

$$a = \frac{n_{10}(\sigma_2 - \sigma_0)}{\tau_1(1/\tau_{10} - 1/\tau_2)} l, \qquad (14)$$

and

$$b = \frac{(\sigma_1 - \sigma_0)\tau_1(1/\tau_{10} - 1/\tau_2)}{\sigma_2 - \sigma_0}. \qquad (15)$$

The pump fluence $F_p$ is related to the initial number density in state 1 by

$$n_{10} = \frac{(1-T_0)F_p}{h\nu\, l}. \tag{16}$$

Substituting (16) into (14), we obtain

$$a = \frac{(1-T_0)(\sigma_2 - \sigma_0)}{h\nu\tau_1(1/\tau_{10} - 1/\tau_2)} F. \tag{17}$$

Since the number of DBBT in state 2 changes the absorption of the sample, it follows that the DFWM signal S satisfies

$$S = An_2^2 = A(e^{-(t-t_0)/\tau_{10}} - e^{-(t-t_0)/\tau_2})^2, \tag{18}$$

with $A$ being a constant that lumps together all the geometric and temporal beam information as well as the field strengths.

We show the fitting to (18) in the DFWM case together with the experimental data in Figure 10. Figure 10(a) shows the detail around the three-beam overlap position ($t = t_0$) and Figure 10(b) shows the long time behavior. The fits to (13) for the pump-probe data are shown in Figure 11(a) and Figure 11(b) respectively for the short and long time response. In doing the fittings, we adopt an iterative routine in which we fit the short time parameters $t_0$, $\tau_{10}$, and $b$ with the short time data and fix them in the long time fitting, and *vice versa*. This process is repeated

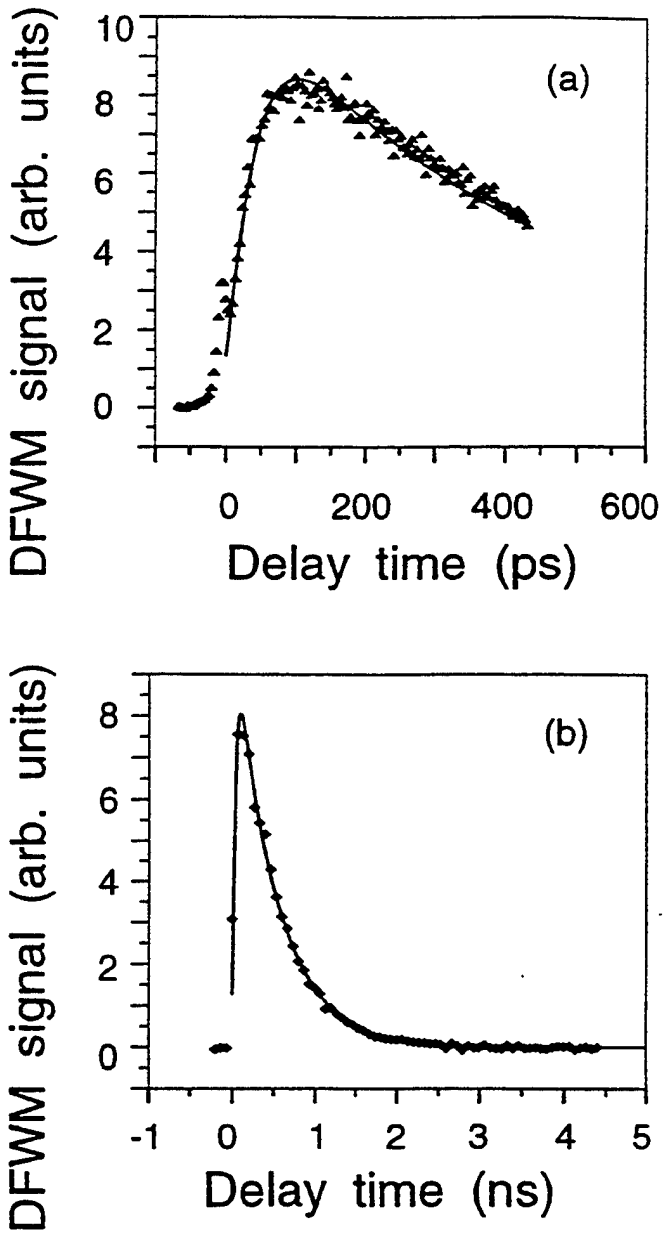


Figure 10. Fittings of the DFWM signal of the doped BBT. (a) Short time response around the three-beam-overlap position gives detail about the rise. (b) Long time behavior reveals information in the decay. Solid lines in (a) and (b) are best fits according to the three-level model.

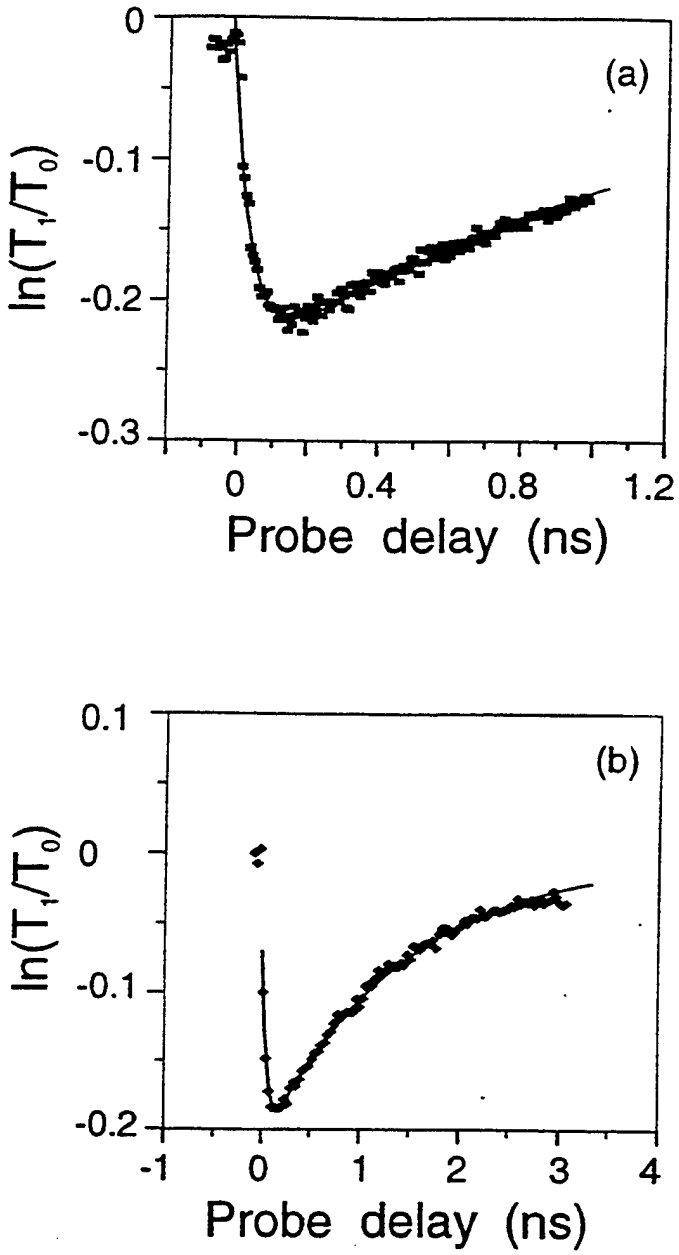


Figure 11. Fitting of the pump-probe data of the doped BBT. (a) Feature around time zero, and (b) the response up to –3 ns for the case of 217mJ/cm$^2$ in the pump beam F. Solid lines fit the data to the three-level model explained in the text.

several times until good agreement in both short and long time fittings is achieved. This process is necessary since the short time response does not contain enough long time information and the long time data can not accommodate the short time detail, as can be seen in Figure 10 and Figure 11. The result from these fittings is organized in Table 3.

Table 3. Fitting results to the three-level model.

| Sample | $\tau_{10}$(ps) | $\tau_2$(ps) | $a$ | $b$ | $t_0$(ps) |
|---|---|---|---|---|---|
| DFWM | 32.31 | 996.5 | / | / | -14.2 |
| Pump-probe | 49.75 | 1419 | 0.2158 | 0.1121 | -14.1 |

From the expressions of $a$ and $b$, one can easily see that both $a$ and $b$ must be positive if the excited-state absorption cross-sections are to be larger than that of the ground state. The buildup and decay in our pump-probe data further indicate that $b$ must be smaller than 1. This is confirmed by the fitting.

We can calculate the time $t_m$ when the transmission reaches its minimum by nullifying the derivative of (13) with respect to time. This gives

$$t_m = t_0 + \frac{\ln[(1-b)\tau_2/\tau_{10}]}{1/\tau_{10} - 1/\tau_2}, \qquad (19)$$

and a relation

$$-\ln(T_1/T_0)\big|_{\min} = \frac{\tau_{10}(1-T_0)(\sigma_2-\sigma_0)e^{-(t_m-t_0)/\tau_2}}{h\nu\tau_1}F. \qquad (20)$$

Equation (20) tells us that $-\ln(T_1/T_0)|_{min}$ is proportional to the pump fluence $F$ with a slope that is the product of a constant and the absorption cross-section difference $(\sigma_2 - \sigma_0)$ between state 2 and the ground state 0. We plot $-\ln(T_1/T_0)|_{min}$ against the pump fluence $F$ in Figure12. The solid line fits the data to (20) and gives

$$\frac{\tau_{10}(1-T_0)(\sigma_2-\sigma_0)e^{-(t_m-t_0)/\tau_2}}{h\nu\tau_1} = 1.011 cm^2/J. \qquad (21)$$

Our sample has a low intensity transmission of 0.18 and a total number density of $1.75\text{x}10^{18}/\text{cm}^3$. This gives a ground state absorption cross-section of $\sigma_0 = 9.76\times10^{-18}\ cm^2$. From the fitting results in Table 3, we find $\sigma_2 - \sigma_0 = 5.25\times10^{-19}(1+\tau_1/\tau_0)\ cm^2$. This experiment does not give clues to the value of $\tau_1/\tau_0$. Therefore the complete determination of the excited-state absorption cross-sections awaits further information regarding the branching ratio of state 1. We can consider the extreme case when all the DBBT in state 1 go to state 2. We have $\tau_1/\tau_0$–0 in this case and $\sigma_2$=$1.03\text{x}10^{-17}$ $\text{cm}^2$, a 5% bigger $\sigma_2$ compared to the ground state $\sigma_0$.

The fitting results in Table 3 indicate a –45% increase in both $\tau_{10}$, and $\tau_2$. To resolve this inconsistency, we study the photon absorption length in our sample. The quantity $1/N\sigma_0$ represents the average distance a photon travels before being absorbed by a DBBT molecule. The quantity $l/(1/N\sigma_0) = N\sigma_0 l$ tells us how many times a photon is likely to be absorbed before it exits the sample. With our 1 mm cell, we find $N\sigma_0 l = 1.7$. In other words, a re-emitted photon still has 70% chance of being absorbed before leaving the sample if it travels in the same direction. A more detailed

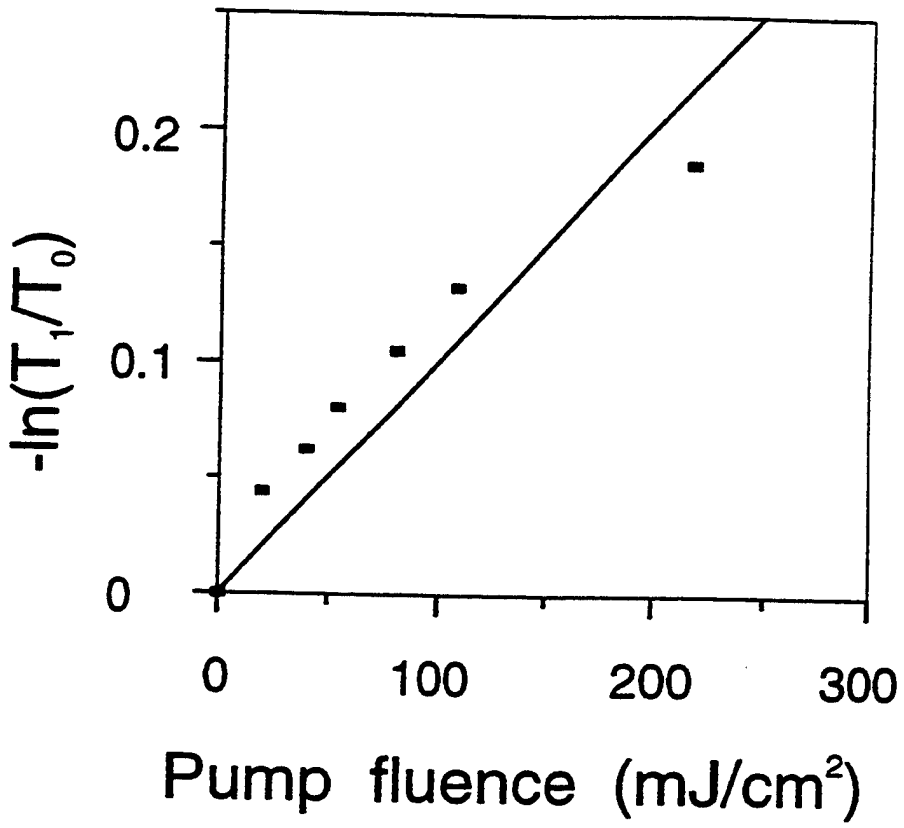


Figure 12. Pump fluence dependence of $-\ln(T_1 / T_0)$. The data are taken at the transmission minimum point. The solid line is the best fit and gives a value $\sigma_2 - \sigma_0 = 5.25 \times 10^{-19}(1+\tau_1/\tau_0)\ cm^2$ for the absorption cross-section difference at 532 nm between state 2 and the ground state 0.

mathematical model involving the random re-emission of a captured photon can be formulated to treat this problem more accurately. Nevertheless the physical picture remains the same. We will not pursue this more exact treatment at this time.

Now let us consider the effect of the trapping of a photon. In the DFWM case, the re-absorption can happen anywhere and the average result is a homogeneous re-population of the excited-state. This re-population will not reinforce the grating that deflects light into the DFWM signal direction and thus the decay time constants remain the same as if there is no photon trapping. In the pump-probe case, there is no grating involved. The re-population of the excited-state makes the DBBT molecules seemingly live longer in both state 1 and state 2 thus lengthening the decay constants $\tau_{10}$, and $\tau_2$. The lengthened decay constants in the pump-probe data can thus be attributed to the photon trapping effect.

In summary, we have demonstrated the success of interpreting both our DFWM and pump-probe date by a three-level model in DBBT. The general agreement between the model and the data is shown. The seemingly puzzling data in the cross-polarized DFWM data is explained by the polarization dependent transition from state 1 to state 2. The lengthening in the decay constants is attributed to the photon trapping effect. We determine the absorption cross-section difference between the excited-state 2 and the ground state 0 to within a branching ratio of the excited-state 1. In the extreme case when no DBBT in state 1 returns to the ground state directly, the absorption cross-section of state 2 is only 5% larger than that of the ground state.

## References


1. C.W. Spangler, and K. O. Havelka, *Materials for Nonlinear Optics*, Eds. by S. Marder, J. Sohn, and G. Stucky, Chapt. 44, (Washington, 1991).

2. X. F. Cao, J. P. Jiang, R. W. Hellwarth, L. P. Yu, M. Chen, L. Dalton, SPIE Proc. **V1337**, 114 (1990).

3. C. W. Spangler, P. K. Liu, and K. O. Havelka, J. Chem. Soc. Perkin Trans. **2**, 1207 (1992).

4. C. W. Spangler, and P. K. Liu, J. Chem. Soc. Perkin Trans. **2**, 1959 (1992).

5. C. W. Spangler, P. K. Liu, A. A. Dembek, and K. O. Havelka, J. Chem. Soc. Perkin Trans. **1**, 799 (1991).]

6. M. Logdlund, P. Dannetun, S. Stafstrom, W. R. Salaneck, M. G. Ramsey, C. W. Spangler, C. Fredriksson, and J. L. Bredas, Phys. Rev. Lett. **70**, 970 (1993).

7. P. Dannetun, M. Logdlund, C. W. Spangler, J. L. Bredas, and W. R. Salaneck, J. Phys. Chem. **98**, 2853 (1994).

8. C. W. Spangler, M. Q. He, J. Laquindanum, L. Dalton, N. Tang, J. P. Partanen, and R. Hellwarth, Mat. Soc. Symp. Proc. **V328**, 655 (1994).

9. C. W. Spangler, M. He, E. G. Nickel, J. Laquindanum, L. R. Dalton, N. Tang, and R. Hellwarth, Mol. Cryst. Liq. Cryst. **240**, 17 (1994).

10. C. W. Spangler, T. J. Hall, K. O. Havelka, M. Badr, M. R. McLean, and L. R. Dalton, SPIE Proc. **V1147**, 149 (1989).

11. J. Swiatkiewicz, M. E. Orczyk, P. N. Prasad, C. W. Spangler, and M. He, SPIE Proc. **V2025**, 400 (1993).

12. J. R. Tallent, R. R. Birge, C. W. Spangler, and K. O. Havelka, *Molecular Electronics-Science and Technology*, ed. A. Aviram, pp. 191-203, (American Institute of Physics, New York, 1992).

13. C. P. de Melo, and R. Silbey, Chem. Phys. Lett. **140**, 537 (1987).

14. C. P. de Melo, and R. Silbey, J. Chem. Phys. **88**, 2567 (1988).

15. A. J. Heeger, S. Kivelson, J. R. Schrieffer, and W. P. Su, Rev. Mod.Phys. **60**, 781 (1988).

16. C. C. Han, and R. L. Elsenbaumer, Syn. Met. **30**, 123 (1989).

17. M. J. Rice, Phys. Lett. **71A**, 152 (1979).

18. J. C. Chiang, and A. G. Macdiarmid, Syn. Met. **13**, 193 (1986).

19. H. Reiss, J. Phys. Chem. **92**, 3657 (1988).

20. J. P. Hermann, D. Ricard, and J. Ducuing, Appl. Phys. Lett. **23**, 178 (1973).

21. J. P. Hermann, J. Ducuing, J. Appl. Phys. **45**, 5100 (1974).

22. K. C. Rustagi, and J. Ducuing, Opt. Commun. **10**, 258 (1974).

23. S. Mukamel, and H. X. Wang, Phys. Rev. Lett. **69**, 65 (1992).

24. J. R. Heflin, K. Y. Wong, O. Zamani-Khamiri, and A. F. Garito, Phys. Rev. B **38**, 1573 (1988).

25. J. R. Heflin, K. Y. Wong, O. Zamani-Khamiri, and A. F. Garito, Mol. Cryst. Liq. Cryst. **160**, 37 (1988).

26. P. N. Butcher, and D. Cotter, *The Elements of Nonlinear Optics*, (Cambridge University Press, New York, 1990).

27. H. A. Bethe, and E. E. Salpeter, Quantum Mechanics of One- and Two- electron Systems, Handbuch der Physik Band XXXV, Atoms I, (Springer-Verlag, Berlin 1957).

# Appendix A

## Synthesis, Procedure and Characterizations: Chemical Doping Studies of Some Novel Ladder Type Heteroaromatic Nonlinear Optical Chromophores

Samuel-Shajing J. Sun, Larry R. Dalton and Zhixin Yang
Department Of Chemistry, University of Southern California
Los Angeles, California 90089-1062

Nansheng Tang, Jouni P. Partanen and Robert W. Hellwarth
Department Of Physics, University of Southern California
Los Angeles, California 90089-0484

Charles W. Spangler and Mingqian He
Department of Chemistry, Northern Illinois University
DeKalb, Illinois 60115

### Abstract

Some novel symmetric donor substituted (push-push) ladder type heteroaromatic 3rd order nonlinear optical(NLO) chromophores, 3, 10 diethoxy - 6, 13 - dibromo - triphenodithiazine (TPDT, or **9**), 6, 6'- bis(2'ethylhexoxy)- 2,2'-bisbenzothiazole (BBT, or **10**), 3, 9, 14 - tris (2'-ethylhexoxy)trithiazine (TTZ, or **11**) are synthesized, characterized, and chemical doping studies employing NMR, EPR, UV-VIS-NIR, photoluminescence and MS spectroscopic techniques indicate these heteroaromatic chromophores have different electronic and optical properties in their radical (soliton) or radical cation (polaron) states. Preliminary picosecond laser Degenerate Four Wave Mixing (DFWM) measurements show these chromophores give out very large resonance enhanced (10-29 to 10-31 esu) second molecular hyperpolarizability (SMH) or $10^{-10}$ esu $\mathbf{X}^{(3)}$ for thin film of TTZ) or off resonance ($10^{-31}$ to $10^{-33}$ esu SMH) third order NLO signals. Intense photoluminescence is seen in various forms of BBT. Nonlinear Optical Limiting (NOL) or Reverse Saturable Absorption (RSA) phenomenon is observed in sulfuric acid doped BBT by pump-probe (P-P) technique. Possible mechanisms of chemical doping are addressed.

### Experimental Section and Results

I. Synthesis and characterizations of 5-(2'-ethylhexoxy) -2-aminothiophenol (**6**). Reaction scheme is shown in Figure A-1.

*Note:* Literature citations in this Appendix refer to documents in the References list.

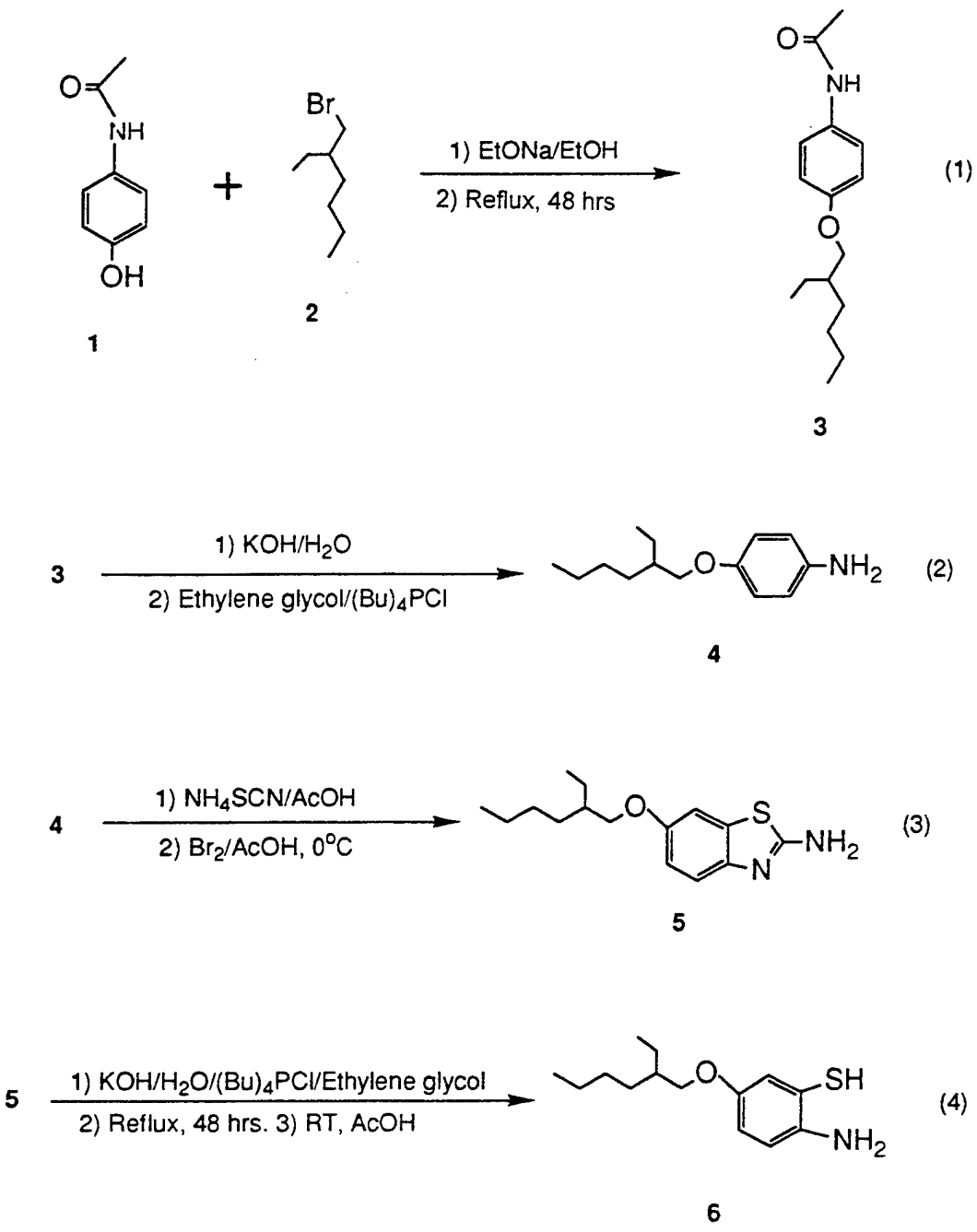


**Figure A-1.** Reaction Schemes

$^1$H NMR spectra were obtained in a Bruker WP200sy FT spectrometer with TMS as internal reference standard. Elemental analyses were performed on a Perkin-Elmer analyzer Model 240 by Paulanne Rider. Melting points were determined by using a Thomas Hoover capillary melting point apparatus that was not corrected.

4-(2'-ethylhexoxy)acetanilide (**3**):

Sodium chips (12.7 g, 0.55 mol) were added to 300 mL ethanol. After all sodium disappeared, 4-acetamidophenol **1** (83.5 g, 0.55 mol) was dissolved in the above solution, 1-bromo-2-ethyl hexane **2** (98 mL, 0.58 mol) was then added dropwise to the solution. The resulting mixture was refluxed for 48 hours and cooled to room temperature. After filtration, the solvent was evaporated and the residue was dissolved in ethyl ether. The organic solution was washed by brine (40 mL x 3) and dried with $MgSO_4$. After removal of solvent, the crude product was obtained (138.6 g, 95%). It was purified from recrystallization in ethanol to give **3** (110.9 g, 76%). Mp: 79-81 °C. $^1$ H NMR in $CDCl_3$: δ 0.86 (m, 6H), 1.2-1.5 (m, 8H), 1.63 (m,1 H), 2.0 (s, 3H), 3.79 (d, J=6.004Hz, 2H), 6.87(d, J=8.005Hz, 2H), 7.44 (d, J=8.005Hz, 2H).

4-(2'-ethylhexoxy)aniline (**4**):

Potassium hydroxide (46 g, 0.82 mol) was dissolved in 50 mL water. The solution was mixed with **3** (103 g). Ethylene glycol (70 mL) and tetrabutylphosphonium chloride (1 g) were added and the resulting mixture was refluxed 24 hours, then poured into water (1000 mL). The organic product was extracted by ethyl ether(3 x 150 mL). The ether solution was washed by brine (3 x 50 mL) and dried over $MgSO_4$. After solvent removal, the pure product 4 was obtained by vacuum distillation, bp. 130°C/1 mmHg yielding **4** (71 g, 82%). $^1$H NMR in $CDCl_3$: δ 0.86 (m, 6H), 1.2-1.5 (m, 8H), 1.63 (m, 1H), 3.91 (d, J=6.004Hz, 2H), 3.74 (s, 2H), 6.49 (d, J=8.005Hz, 2H), 6.63(d, J=8.005Hz, 2H). Elemental analysis found (%): C(75.65), H(10.73), N(6.25). Calculated for $C_{14}H_{23}NO$ (%): C(75.97), H(10.47), N(6.32).

2-Amino-6-(2'-ethylhexoxy)benzothiazole (**5**):

To a solution of **4** (71 g, 0.32 mol), ammonium thiocyanate (195 g, 2.57 mol) dissolved in 300 mL glacial acetic acid, bromine (103 g, 0.64 mol) dissolved in 120 mL AcOH were added dropwise at 0°C. After the addition was complete, the mixture was stirred at room temperature overnight. The crude product was obtained by filtration and was recrystallized in methanol to obtain the pure 5(76.5 g, 89.5%). Mp. 133-135°C. $^1$H NMR in $CDC1_3$: δ 0.86 (t, 6H), 1.2-1.5 (m, 8 H), 1.63 (m, 1 H), 3.85 (d, J=6.204 Hz, 2H), 5.26 (s, 2 H), 6.92 (d, J=8.405 Hz,1 H), 7.13 (s, 1H), 7.44 (d, J=8.606 Hz, 1H). Elemental analysis found (%): C (64.76), H (8.00), N (10.07), S (11.49). Calculated for $C_{15}H_{22}N_2OS$: C (64.75), H (7.91), N (10.01), S (11.51).

5-(2'-ethylhexoxy)-2-aminothiophenol (**6**):

Compound **5** (43 g, 0.119 mol) was mixed with potassium hydroxide (100 g, 1.78 mol), 60 mL water, 1.0 g tetrabutylphosphonium chloride, and ethylene glycol (30 mL). The mixture

was refluxed for 48 hours. It was then cooled to room temperature and neutralized with AcOH(5N). The product was extracted with ethyl ether(3 x 100 mL). The organic solution was washed with saturated sodium bicarbonate, brine, and then dried over magnesium sulfate. The solvent was evaporated and compound **6** was obtained as a liquid (28 g, 71.5%). $^1$H NMR in $CDCl_3$: δ 0.86 (t, 6H), 1.2-1.5 (m, 8H),1.63 (m, 1H), 3.58 (d, J=5.664 Hz, 2H), 4.03 (s, 3H), 6.63-6.81(m, 3H). Elemental analysis found (%): C (66.51), H (9.19), N (5.53), S(12.91). Calculated for $C_{14}H_{23}NOS$ (%): C (66.40), H (9.09), N (5.54), S (12.65).

II. Synthesis and characterizations of 3, 10 - diethoxy - 6, 13 - dibromo - triphenodithiazine (TPDT, **9**), 6, 6'- bis(2'- ethylhexoxy)- 2,2'-bisbenzothiazole (BBT, **10**) and 3, 9, 14 - tris(2'-ethylhexoxy)- trithiazine (TTZ, **11**). (Reaction schemes are shown in Figure A-2.)

Reagents and solvents were purchased commercially, and used without further purification unless otherwise noted. Bromanil (purchased from Aldrich) was recrystallized from 95% ethanol. Melting points were measured using capillary tubes on a Mel-Temp apparatus and are uncorrected. Proton and carbon NMR spectra were taken using a Bruker-250 spectrometer operating at 250 MHz, with tetramethylsilane (TMS) internal standard reference for chemical shift. FTIR spectra were obtained using a Perkin-Elmer 1760 FTIR spectrophotometer. UV-VIS-NIR spectra were obtained using a Perkin-Elmer Lambda-4C UV-VIS spectrophotometer. EPR measurements were carried out on an IBM ER 200D-SRC ESR spectrometer. Luminescence spectra were obtained on a Perkin-Elmer LS-5 luminescence spectrophotometer. Elemental analyses were performed by Atlantic Microlab Inc. MS analyses were done at UC Riverside Mass Spectra Facility.

6, 6'- bis(2'- ethylhexoxy)- 2,2'-bisbenzothiazole(**10**), 3, 9, 14 - tris(2'ethylhexoxy)- trithiazine (**11**):

A modified method for the synthesis of smaller derivatives of **11**[13] is employed here.

p-Bromanil (2.17 g, 5.12 mmol) was mixed with 2.0 g sodium acetate, 25.0 mL 0.68 M (17.0 mmol) **6** in DMF were added to the mixture in a dry and inert gas-filled reaction flask. The mixture immediately turned dark. The reaction mixture was refluxed at 150-155°C under inert gas; the progress of reaction was monitored by TLC with toluene as elute solvent. (The top violet spot was **11** and the 2nd luminescent spot was **10**.) The reaction was stopped after 18 hours. The product mixture was vacumm dried in a Rotovac™ and then redissolved in 20 mL toluene. This violet colored toluene solution was then washed with D.I.water several times until the water phase became clear. The toluene phase was dried with calcium hydride, then the product mixture was eluted on a silica gel column with toluene as e!ute solvent. The first violet fraction was **11**. After toluene was removed by vacuum Rotovac, about 0.8 g (20% yield) violet sticky gel **11** was obtained. The second white-blue and luminescent (under 356 nm UV) fraction was **10**; after drying, about 50 mg crystal remained. The thin layer crystal **10** spread on the inside walls of the flask displayed an intense yellow luminescence under 356 nm UV light. Chromophore **10** can also be prepared without the presence of p-bromanil, i.e., by refluxing **6** in DMF at 150-155 °C; however, sodium acetate must be present in order to initiate the the reaction.

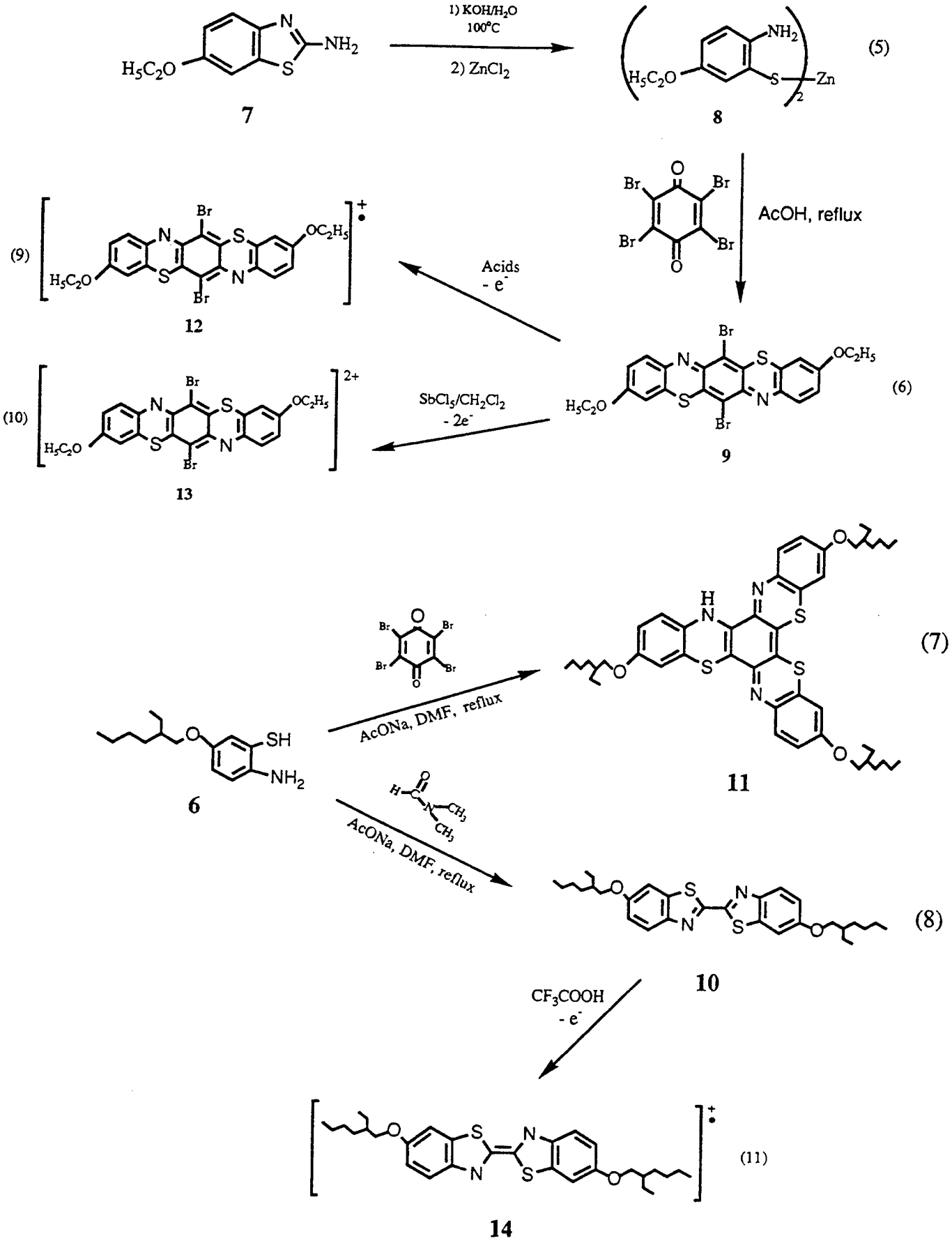


**Figure A-2.** Reaction Schemes

$^1$H NMR of **11** in $CDCl_3$ (Figure 3): δ 0.8-1.0 (m, 18H), 1.2-1.5 (m, 24H), 1.5-1.8 (m, 3H), 3.60 (d, J=5.85Hz, 2H), 3.65 (d, J=5.81 Hz, 2H), 3.73 (d,J=5.76Hz, 2H), 6.16 (d, J=8.50 Hz, 1H), 6.24 (m, 1H), 6.33 (d, J=2.40 Hz, 1H), 6.48 (m, 2H), 6.57 (d, J=2.51 Hz, 1H), 6.65 (m, 1H), 7.10 (d, J=9.57 Hz, 2H), 7.33 (d, J=8.80 Hz, 1 H). 1H NMR of 11 in CF3COOD:δ 0.8-1 .2 (s, br, 6H), 1.2-1 .8 (s, br, 8H), 1.8-2.0 (m, br, 1H), 3.8-4.2 (br, small), no more aromatic protons. $^{13}$C NMR of **11** in $CDCl_3$ (Figure 4): δ11.0, 14.1, 23.0, 23.7, 28.9, 30.2, 39.2, 70.9, 77.2,108.9, 109.5, 110.2, 111.0, 112.2, 112.8, 114.2, 114.8, 115.3, 119.9, 122.5, 124.4, 131.3, 132.0, 132.2, 132.7, 133.9, 136.3, 137.0, 140.4, 155.3, 157.7, 158.7. FAB-MS of 11(Figure 5): major peaks: 825 (50%), 824 (100%), 712 (36%), 711(20%), 599(13%), 598(13%), 486 (31%), 485 (11%). Calculated: 824.2 ($C_{48}H_{61}N_3O_3S_3$, molecular formula), 711.0 (one -$C_8H_{17}$ side chain was lost), 598.0(two -$C_8H_{17}$ side chains were lost), 484.6 (molecule lost all three -$C_8H_{17}$ side chains). UV-VIS spectra of 11 in dichloromethane: 340nm (0.54), 550 nm (0.42, shoulder peak), 590 nm (0.60), are shown in Figure 6 (including medium such as TFA).

$^1$H NMR of **10** in $CDCl_3$ (Figures 7 and 8): δ 0.8-1.0 (m, 12H), 1.2-1.6(m, 16H), 1.7-1 .9 (m, 2H), 3.91 (d, J = 5.72 Hz, 4H), 7.13 (q, 2H), 7.38 (d, J = 2.43 Hz, 2H), 7.98 (d, J = 9.02 Hz, 2H). $^{13}$C of (**10**) in $CDCl_3$ (Figures 9 and 10): δ11.1, 14.1, 23.1, 23.9, 29.1, 30.5, 39.4, 71.1, 104.5, 117.0, 124.3, 137.2, 147.9, 158.5, 158.9. $^1$H NMR of **10** in $CF_3COOD$ (Figures 7 and 8): δ 0.8-1.1 (m, 12H), 1.2-1 .7(m, 16H),1.8-2.1 (m, 2H), 4.16 (d, J= 5.68 Hz, 4H), 7.5-7.6 (q, 2H), 7.65(d, J=1.86 Hz, 2H),8.19 (d, J=9.28 Hz, 2H). $^{13}$C of **10** in $CF_3COOD$ (Figures 9 and 10): δ11.6, 14.6, 24.6, 25.4, 30.8, 32.2, 41.4, 74.6, 106.6, 123.8, 124.6, 138.1, 142.6, 155.5, 164.1. FAB-MS (Figure 11) of **10**, major peaks: 525 (17%), 524 (46%), 412 (11%), 301 (22%), 300 (100%), 299 (17%), 267 (11%), 149 (3%), 100 (64%). Calculated: 524.8 ($C_{30}H_{40}N_20_2S_2$, molecular formula), 411.6 (one -$C_8H_{17}$side chain was lost), 298.4 (two -$C_8H_{17}$ side chains were lost), 149.2 (one benzothiazole ring), 99.2 (end -CH2- was lost in -$C_8H_{17}$). Elemental analysis of **10**, found(%): C (68.70), H (7.80). Calculated (%): C (68.67), H (7.68). M.P.=65-67°C. UV-VIS and luminescence spectra data of **10** in different media are tabulated in Table A-1, the representative absorption spectra are depicted in Figure 12 and luminescence (emission) spectra are in Figure 13

**Table A-1.** UV-VIS aborption and emission maxima of **10** in different media.

| | Absorptions maxima | Emission maxima |
|---|---|---|
| Methanol | 370 nm | 444 nm |
| 96% $H_2SO_4$ | 457 nm | 540 nm |
| 99% $CF_3COOH$ | 458 nm | 575 nm |

3, 10 - diethoxy - 6, 13 - dibromo - triphenodithiazine (**9**):

Compound **9** was reported before,[14] and the synthesis of it followed the literature procedure. However, probably due to its poor solubility in organic solvents, no NMR data are available in the literature. Here the $^1H$ spectrum was obtained 20 minutes after **9** was dissolved in $CF_3COOD$ (Figure 13): δ 8.05 (d, J=9.46 Hz, 2H), 7.44 (d, J=9.32 Hz, 2H), 7.35 (s, 2H), 4.35 (tetra, 4H), 1.59 (t, 6.77 Hz, 6H). M.P.>400 °C (a solid phase transition was observed at 325 °C). Elemental analysis of **9**, found (%): C (46.72), H (2.89), Br (28.47). Calculated (%): C (46.83), H (2.86), Br (28.32). VIS absorption maxima of **9** in different media are tabulated in Table A-2, and representative UV-VIS spectra are shown in Figure 14.

**Table A-2.** VIS-NIR absorptions of **9** in different media

| Media | $CH_2Cl_2$ | $CF_3COOH$ (99%) | HCl (37%) | $H_3PO_4$ (85%) | $H_2SO_4$ (96%) | $SbCl_5/CH_2Cl_2$ |
|---|---|---|---|---|---|---|
| $\lambda_{max}$(nm) | 584 | 800 | 805 | 808 | 815 | 835-850 |

Nonlinear optical measurements include degenerate four-wave mixing (DFWM) and pump-probe (P-P) techniques. Carbon disulfide($CS_2$) was used as a reference standard. A 532 nm or 1064 nm laser pulse(derived from 5 Hz repetition rate mode-locked pulses of a Quantel Model YG471-C Nd:YAG laser) has energy of approximately 2 mJ (532 nm) or 10 mJ (1064 nm) in a 1.5 mm diameter beam, a duration of approximately 30 picoseconds. The pulse energy fluctuations were of the order -20% to +20%.

The 2nd molecular hyperpolarizabilities $\gamma_{1111}$ (x $10^{-31}$ esu) at both 532 and 1064 nm are tabulated in Table A-3. Details of measurements and calculations are to be reported separately.[15]

**Table A-3.** $\gamma_{1111}$ (x $10^{-31}$ esu) at 532 and 1064 nm fundamental radiation

| | 532 nm | | | 1064 nm |
|---|---|---|---|---|
| | Organic solvent | $CF_3COOH$ | $H_2SO_4$ | $H_2SO_4$ |
| 11 | 8.2 | ND* | ND | ND |
| 10 | 6.8 | 0.9 5 | 1.4 | N D |
| 9 | 1 5 0 | 2.4 | 3.0 | 0.0 21 |

*ND= Not detectable due to various reasons.

Chromophore **11** was also spin cast from toluene onto microslide to form thin films, and $\chi^{(3)}_{1111}$ = 6.7 x $10^{-10}$ esu was obtained for a film of 0.5-1.0 μm thick.